A 3D Numerical Model of the Electrostatic Coating Process with Moving Mesh Capability and Multiple Passes

N. Toljic[a], K. Adamiak[a], *Fellow IEEE*, G. S. P. Castle[a], *Life Fellow IEEE*, Hong-Hsiang (Harry) Kuo[b] and Hua-Tzu (Charles) Fan[b]

[a] Department of Electrical and Computer Engineering, University of Western Ontario, London, Ontario, Canada
[b] General Motors Company, Michigan, USA

***Abstract*—In this paper, a full three dimensional numerical model of the electrostatic coating process with moving mesh capability and capable of handling multiple target passes is presented. The target follows piecewise linear motion, so that the entire area of the target has been coated twice. All the dominant mechanical and electrical phenomena were taken into account and cases with both neutral and charged particles were examined. It was confirmed that the transfer efficiency increases when the electrical forces are present in the model and that the uniformity improves with the movement of the target.**

I. INTRODUCTION

In practical electrostatic coating applications the target is commonly coated multiple times. The reason for treating the same area of the target in several passes is to increase the level of deposition and also to improve the uniformity. The numerical model of the process needs to be capable of replicating the exact motion pattern of the target, including multiple passes.

A number of published papers describe methods and report results for the numerical simulation of charged particle motion in both liquid and particle coating applications. In the work by Usah et al. [1], numerical modeling of a complete powder coating process was carried out to understand the gas-particle two-phase flow field inside a powder coating booth and the results of the numerical simulation were compared with experimental data to validate the numerical model. Zhao et al. [2], used the commercial program FLUENT to solve the mechanical portion of the spraying process and the user defined functions (UDFs) were used to solve the Poisson equation governing the electric field distribution. Ye et al. [3] presented the results of investigations aiming to numerically simulate the electrostatic powder coating process in the automotive industry. In previous studies, the current authors [4-5] developed a full 3D numerical model of the industrial electrostatic coating process and sample results of its capabilities were demonstrated.

All the calculations in the afore-mentioned papers were performed for the cases with a

stationary target. There have been very few reported attempts to include the effect of motion. In one attempt to deal with this the present authors considered the simulation of moving targets, but the results were based on data from a stationary case using the superposition principle and were only applicable to axially symmetric geometries [6]. The use of a moving mesh for simulation of a one dimensional, linear type motion has been discussed in [7]. It was shown that the re-meshing and smoothing techniques for moving mesh are superior when compared to the layering method (the latter has multiple adjacent layers with different mesh density). So far, the authors have been unaware of any attempts to simulate more complex types of motion in the numerical simulations of the coating process.

The purpose of this research is to develop a full 3D numerical model of the coating process with a moving mesh feature and piecewise linear motion of the target. This is the type of motion most commonly encountered in real applications and is of great practical importance. Here, the target is linearly moving in one direction for some time, making a turn and then linearly reversing (i.e. it follows a piecewise linear trajectory). The pattern is then repeated a sufficient number of times to cover the whole target twice. The mechanical part of the coating process is directly modeled with the computational fluid dynamics software FLUENT. Its User Defined Function (UDF) capabilities are used to solve the Poisson field by incorporating it into the general scalar transport equations within FLUENT. This enables the calculation of the electrostatic force on the charged particles.

The paper is organized in several sections. The first section is introductory and is followed by a description of the computational domain and target movement. The next section presents the results of the discrete phase simulations with both neutral and charged particles. Finally, conclusions are derived.

II. NUMERICAL PROCEDURES

The computational three-dimensional domain encompasses a simplified representation of the rotary atomizer and a perforated plate target with 0.8m in length and 0.6m in width situated 0.25m away from the atomizer. The coating material, which can be either liquid or solid, is fed under high pressure from a supply reservoir to the bell atomizer and then introduced into the atomizer cup. The cup (32 mm in radius) rotates at a high speed (typically of 5,000 to 45,000 rpm). Particles are pushed towards the edge of the cup and ejected in the radial direction. A shroud surrounds the atomizer cup. This shroud provides either an annulus or a number of small holes through which the shaping air is supplied. The role of the shaping air is twofold. Firstly, it is used to assist in creation of particles and their separation from the atomizer. Secondly, it focuses the particle trajectories (hence it's also known as the focusing air). Commonly, the process is modified by connecting a voltage source to the rotating bell, which provides conduction charging of the atomized particles. Here, conduction charging is the predominant mechanism for particle charging and the effects of triboelectrification has been neglected. The numerical algorithm includes solving the gas phase of the shaping air, the discrete phase of the charged particles, the electrostatic field and coupling between them to get a self-consistent solution [8].

The shaping air flow in FLUENT was considered as incompressible, steady and viscous turbulent. The RNG (renormalization group) k-ε turbulent model was used in the modeling. The method used for simulation of the particle discrete phase in FLUENT is

the discrete phase model and is solved by the Lagrangian approach in which the particles are tracked by the stochastic tracking (random walk) model in turbulent gas flow [8]. Coupling between the air flow and the particle discrete phase is included via source terms of mass and momentum. The particles are ejected with the predefined size and charge distribution and directed by the shaping air to the target.

The electric field generated by the voltage applied to the bell cup and the space charge formed by the charged particles is governed by Poisson's equation

$$\nabla^2 \Phi = -\frac{\rho}{\varepsilon_0} \qquad (2.1)$$

where Φ is the electrical potential, ρ is the total space charge density and ε_0 is the permittivity of the air. The electric field intensity $\mathbf{E}$ can be calculated as

$$\mathbf{E} = -\nabla \Phi \qquad (2.2)$$

The Poisson's equation can be solved by the FLUENT solver using user-defined scalar transport equation [8]. The diffusion coefficient and the source term in the FLUENT transport equation are substituted with the electrical permittivity and the total space charge density, respectively.

Total space charge density is given by:

$$\rho = \rho_p + \rho_i \qquad (2.3)$$

where ρ_p is the space charge density of the charged particles and ρ_i is the space charge density of the ions generated due to corona discharge near the bell edge.

The space charge density of the charged particles in a given cell can be expressed as

$$\rho_p = \frac{1}{N} \sum_{k=1}^{N} q_k / m_k \cdot C_k \qquad (2.4)$$

where q_k ,m_k ,C_k are the total charge, mass and concentration of the particles of the given size in the cell, and N is the total number of particles with different sizes.

The space charge density due to the ions can is related to the total current density, which is given by:

$$\mathbf{J} = \rho_p(\mu_p \mathbf{E} + \mathbf{v}_p) + \rho_i(\mu_i \mathbf{E} + \mathbf{v}_i) - D_p \nabla \rho_p - D_i \nabla \rho_i \qquad (2.5)$$

where μ_p and μ_i respectively represent the ion and the particle mobilities, v_p and v_i respectively represent the particle and ion velocities, and D_p and D_i respectively represent the diffusion coefficients for the particles and ions. Since the ion mobility is very large compared to particle mobility and the diffusion coefficients, we can assume:

$$\rho_i \mu_i \mathbf{E} >> \rho_i \mathbf{v}_i + \rho_p(\mu_p \mathbf{E} + \mathbf{v}_p) - D_p \nabla \rho_p - D_i \nabla \rho_i \qquad (2.6)$$

In this case, equation (2.5) can be simplified as:

$$\mathbf{J} = \mu \rho_i \mathbf{E} \qquad (2.7)$$

The total space charge density due to the ions can be expressed from the previous equation as:

$$\rho_i = J / \mu E \qquad (2.8)$$

Since we are considering the process that is steady in time, the total current density satisfies the continuity equation in the following form:

$$\nabla \cdot \mathbf{J} = 0 \qquad (2.9)$$

In order to incorporate the current density, **J,** into the numerical analysis, a new scalar function is introduced and defined as

$$\mathbf{J} = -\nabla \Psi \qquad (2.10)$$

By combining the equations (2.9) and (2.10) we obtain

$$\nabla^2 \Psi = 0 \qquad (2.11)$$

The equation (2.11) can be solved by the FLUENT solver using user-defined scalar transport equation [8]. We will assume that the total corona current at the electrode is known; it is constant at the electrode surface, equal to zero at the other boundaries of the computational domain and its normal derivative is zero at the target surface.

The geometry of the computational domain was created by the ICEM software package [9] and meshed in an unstructured manner. The total number of cells used for meshing is around 500,000. All the volume cells are tetrahedral and all the surface cells (faces) are triangular. The mesh between the atomizer and the target was refined compared to the rest of the computational domain. The computational domain is shown in Figure 1. The door target takes the shape of a plate (0.8m in length, 0.6m in width and with 0.01m thickness) with a hole for the handle. Initially, the target is positioned so that its centre is 0.4m away from the atomizer centerline in the negative *x* direction and 0.3m away from the atomizer centerline in the negative *y* direction. The target is linearly moving in the *x* direction, making a turn in the negative *y* direction, linearly reversing, again making a turn and then repeating the motion in a number of passes (Figure 2). At the moment when the entire area of the target is coated, the target starts translation in the negative *y* direction with a uniform velocity of 0.4m/s for the duration of 0.375s. Upon completion of this movement, the process is repeated in the reversed order.

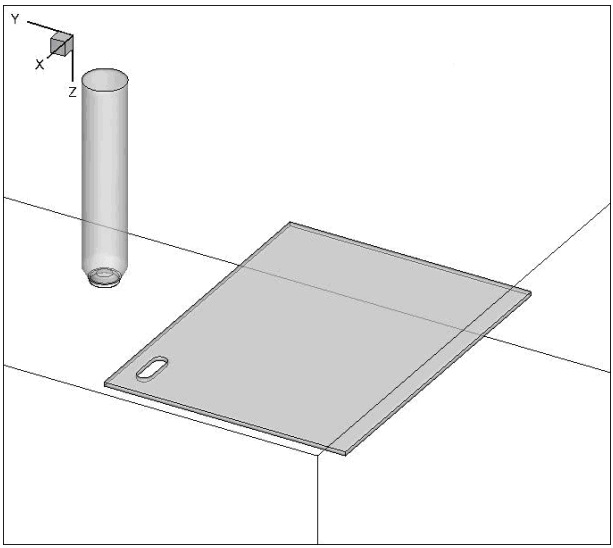

Fig. 1. Initial computational domain

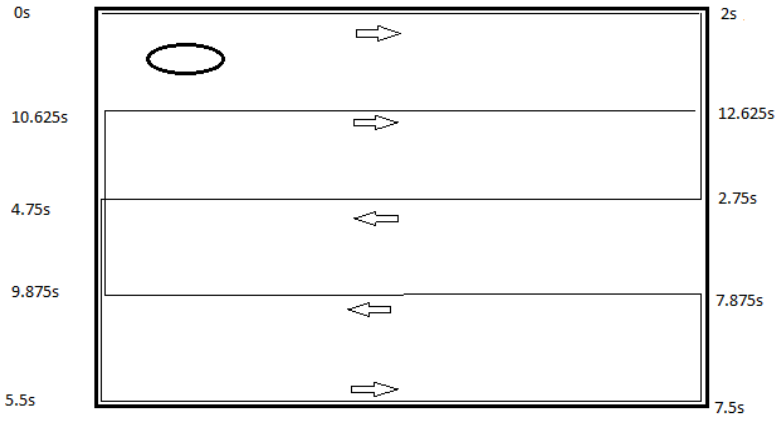

Fig. 2. Motion pattern of the gun relative to the target

III. NUMERICAL RESULTS

In all calculations, the shaping air flow rate was set to be 0.02 kg/s. The atomizer voltage was assumed to be -90kV, whereas the target was grounded. The value of the charge-to-mass ratio is set to be inversely proportional to the particle radius and equal to -1mC/kg for the particle with 35μm diameter [10]. The corona current has been determined experimentally for the case when particles are present as 10μA. The base values for the particle size distribution and the corresponding flow rates are given in the Table 1 [11].

TABLE 1: PARAMETERS OF THE PARTICLE SIZE DISTRIBUTION

Particle diameter[μm]	Flow rate[g/s]
10	0.03
15	0.15
20	0.36
25	0.6
30	0.84
35	0.9
40	0.81
45	0.588
50	0.45
55	0.39
60	0.24
65	0.186
70	0.168
75	0.15
80	0.138

A. Discrete phase modeling with neutral particles

In this section, the results of discrete phase modeling with neutral particles are presented. Sampling of the particle trajectories in the time equal to 0s is shown in the Figure 3. The atomizer is positioned directly above a corner of the target. Particles form a cone in the region between the atomizer and the target as they get ejected from the atomizer tip. It can be seen that a large number of particles bypass the target. Some of the particles hit the target or move along the target.

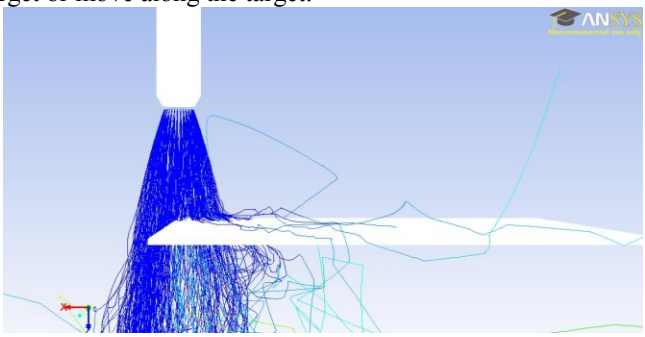

Fig. 3. Sampling of particle trajectories for time equal to 0s

The contours of the accumulation for time equal to 1s are given in Figure 4. At this moment, the atomizer is directly above the middle of the longer edge of the target. The first half of the first pass is already completed and this is reflected in the deposition pattern. The area around the perforation exhibits higher deposition.

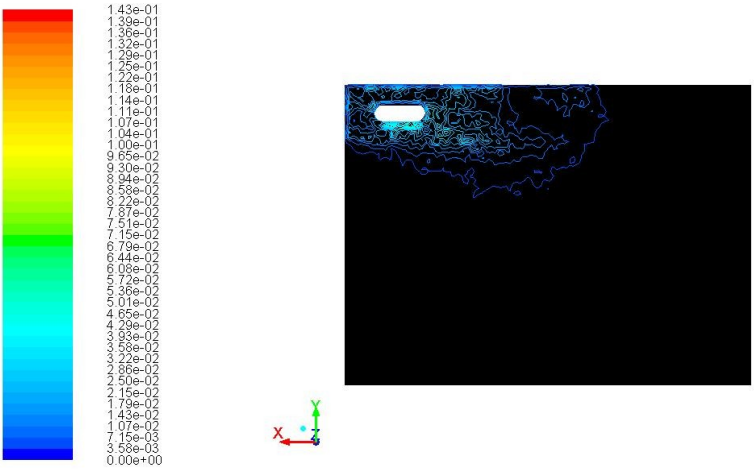

Fig. 4. Contours of the accumulation [kg/m^2] for time equal to 1s

The contours of the accumulation for time equal to 8s are given in Figure 5. At this moment, the entire area of the target has been coated and the target starts the reversing mo-

tion. The particle deposition pattern reflects the motion of the target. The uniformity is considerably improved, but there are areas with relatively high deposition.

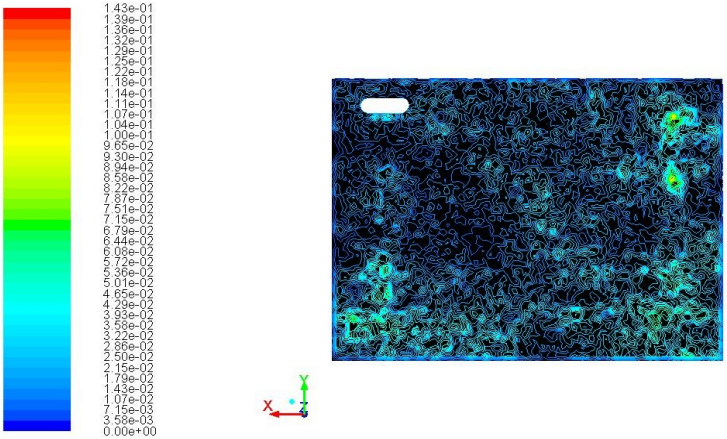

Fig. 5. Contours of the accumulation [kg/m^2] for time equal to 8s

The contours of the accumulation for time equal to 13s are given in Figure 6. At this moment, the reversed motion of the target has been completed and the target has been coated for the second time. Uniformity is significantly improved, although there are still scattered parts with very high deposition. Areas around the perforations also exhibit larger values of deposition. The transfer efficiency calculated as the ratio of the deposited mass flow rate and the input mass flow rate is approximately equal to 60%.

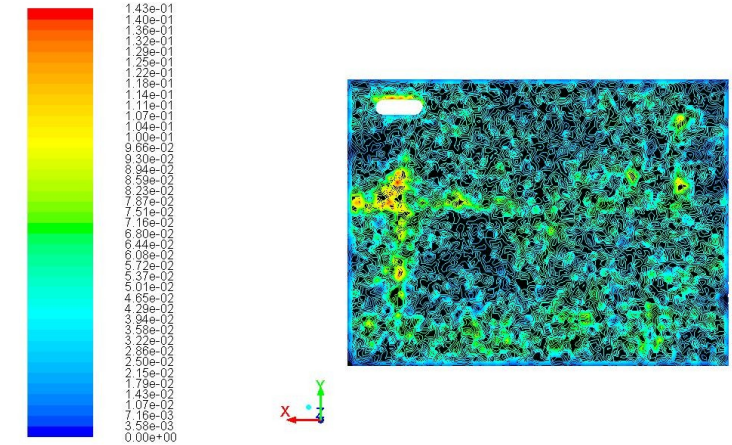

Fig. 6. Contours of the accumulation [kg/m^2] for time equal to 13s

B. Discrete phase modeling with charged particles

In this section, discrete phase modeling with charged particles is presented. Atomizer is connected to a high voltage power supply of -90kV and the corona current

is10μm. Sampling of the particle trajectories in the time equal to 0s is shown in the Figure 7. Similarly to the case with no electric charge, particles form a cone in the region between the atomizer and the target as they get ejected from the atomizer tip, and the conical stream of particle partially bypasses the target. Some of the particle trajectories are deflected towards the back of the target due to the wrap around effect.

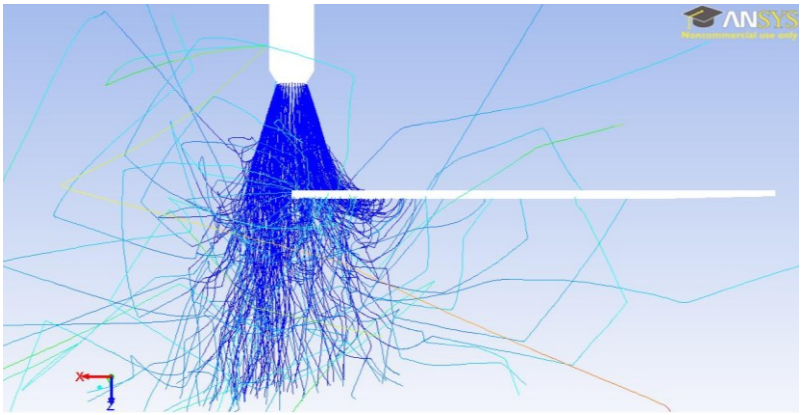

Fig. 7. Sampling of particle trajectories for time equal to 0s

The contours of the accumulation for time equal to 1s are given in Figure 8. The first half of the first pass is finished which is reflected in the deposition pattern. By comparing raw output data, it can be concluded that the deposition is larger compared to the case with neutral particles which is explained by the presence of the attraction forces between the particles and the target.

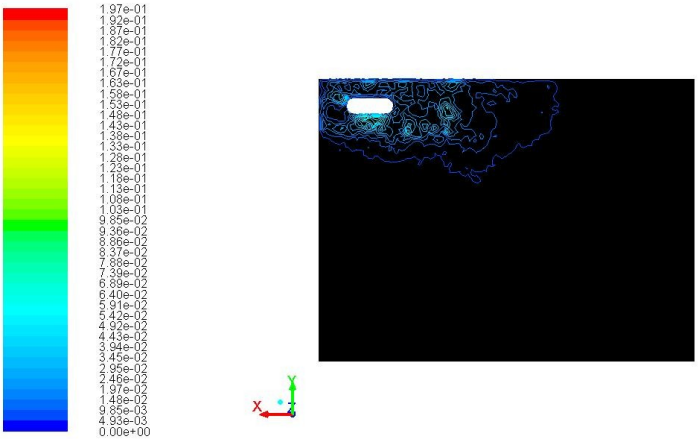

Fig. 8. Contours of the accumulation [kg/m^2] for time equal to 1s

The contours of the accumulation for time equal to 8s are shown in the Figure 9. At this moment, the entire area of the target has been coated once. Again, by comparing the out-

put data, it can be noted that the deposition is larger when compared to the case with neutral particles. Certain regions of the target exhibit much larger than average values of deposition.

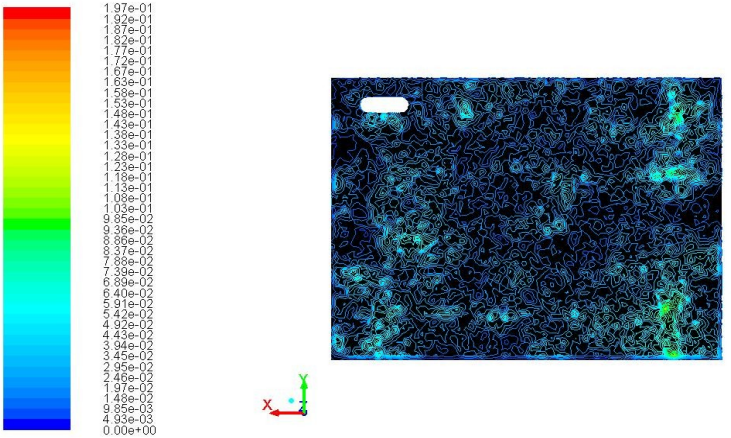

Fig. 9. Contours of accumulation [kg/m^2] for time equal to 8s

The contours of the accumulation for time equal to 13s are given in Figure 10. The target has completed the reversed motion and the entire area of the target has been coated once again. The transfer efficiency calculated as the ratio of the deposited mass flow rate and the input mass flow rate is approximately equal to 75% which is increased comparing to the case with neutral particles. Certain regions of the target exhibit improved uniformity and deposition. The deposition around perforations remains at a higher level due to the edge effects (window panning).

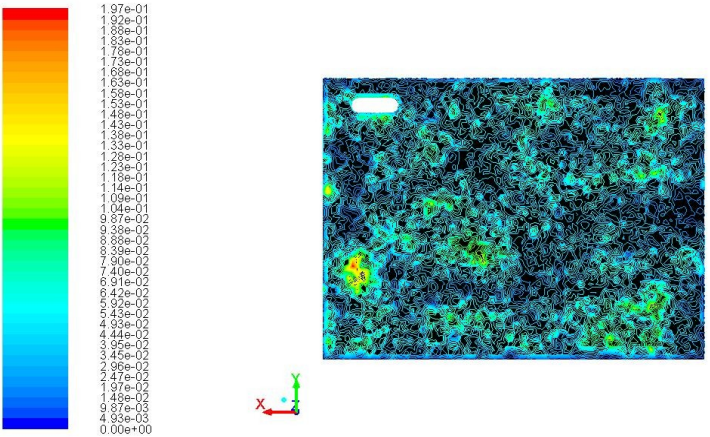

Fig. 10. Contours of the accumulation [kg/m^2] for time equal to 13s

IV. Conclusion

In this paper, a full 3D numerical model of the electrostatic coating process with moving mesh feature and multiple passes has been presented. The mechanical part was directly modeled with the computational fluid dynamics software, FLUENT. Its user-defined functions were used to solve the Poisson field by incorporating it into the general scalar transport equations within FLUENT. Coupling between the airflow phase, the particle discrete phase and the electrostatic field yields the trajectories of the charged particles. It has been demonstrated that the moving mesh feature for the FLUENT numerical model of the electrostatic coating process can successfully simulate multiple passes. The entire area of the target has been treated twice, which is reflected in the deposition pattern. Cases with neutral and charged particles are examined. When the particles are charged, the transfer efficiency increases compared to the case with neutral particles. It has been discovered that for the current setup of the simulation parameters, the uniformity improves with the progression of the target, but only to a lesser degree. A separate investigation on the accuracy of the solution suggests that the uniformity improves dramatically when the density of the mesh is increased. Additional future studies are recommended in order to clarify the influence of other factors (e.g. number of injections, distribution of superparticles, etc.) on the deposition uniformity.

V. Acknowledgment

The authors acknowledge with thanks the joint contributions of National Science and Engineering Research Council of Canada and General Motors Company for the financial support in aid to this project.

References

[1] U. Shah, J. Zhu, C. Zhang, F. Wang, R. Martinuzzi, Validation of a numerical model for the simulation of an electrostatic powder coating process, *Int. J. of Multiphase Flow* 33 (2007) 557-573.

[2] S. Zhao, K. Adamiak, G.S.P. Castle, The implementation of Poisson field analysis within FLUENT to model electrostatic liquid spraying, 2007 IEEE Canadian Conference on Electrical and Computer Engineering, Vancouver, Apr. 22-25, 2007.

[3] Q. Ye, J. Domnick, On the simulation of space charge in electrostatic powder coating with a corona spray gun, *Powder Technol*. 135 (2003) 250–260.

[4] N. Toljic, G. S. P. Castle, K. Adamiak, H. H. Kuo, C. T. Fan, Three-dimensional numerical studies on the effect of the particle charge to mass ratio distribution in the electrostatic coating process, *J. Electrostatics* (accepted for publication).

[5] N. Toljic, G. S. P. Castle, K. Adamiak, H. H. Kuo, C. T. Fan, Incorporation of the corona current into a numerical 3D model of the electrostatic coating process, *J. Part. Sci. Tech*. (accepted for publication)

[6] N. Toljic, G. S. P. Castle, K. Adamiak, H. H. Kuo, C. T. Fan, A 3-D numerical model of the electrostatic coating process for moving targets, *Proc. 13th International Conference on Electrostatics*, April 2011, Wales, UK

[7] Q. Ye, Using dynamic mesh models to simulate electrostatic spray-painting, *High Performance Comp. Sci. Eng*. 5 (2006) 173-182.

[8] FLUENT User's Guide, www.fluent.com

[9] ICEM User Manual, www.ansys.com

[10] N. Toljic, G. S. P. Castle, K. Adamiak, Charge to radius dependency for conductive particles charged by induction, *J. Electrostatics* 68 (2010) 57-63.

[11] UWO-GM Internal Correspondence, 2009.